M. OTTE (éd.), **Nature et Culture**, Colloque de Liège (13-17 décembre 1993), Liège, E.R.A.U.L. 68, 1995, p. 667 à 681.

HIGH-RESOLUTION COMPUTED TOMOGRAPHY AND MICRO-FOCUS RADIOGRAPHY ON AN EIGHT THOUSAND YEAR OLD PLASTERED SKULL : HOW AND WHY IT WAS MODELED

I. HERSHKOVITZ, I.ZOHAR et S. WISH-BARATZ[1]

Y. GOREN et N. GORING-MORRIS[2]

M.S. SPEIRS[3]

I. SEGAL[4]

O. MEIRAV et U. SHERTER[5]

H. FELDMAN[6]

INTRODUCTION

Plastered skulls are among the most dramatic finds and fascinating religious artifacts to have been discovered. They first appeared in the Levant in the Pre-pottery Neolithic B period, 7300 - 6000 B.C. (PPNB). During this period mankind made a leap forward in the direction of modern society with a transition in the subsistence mode from hunting and gathering to an agriculturally based economy (Bar Yosef and Belfer-Cohen, 1989a,b). At that time, human skulls were removed from their burials, plastered, decorated and finally set in shrines, most likely for ritualistic purposes (Hershkovitz and Gopher, 1990). In every site where plastered skulls were found, i.e. Ein Ghazal, Jericho, Munhata, Tel Ramad, Nahal Heimar and K'far Hahoresh different styles of plastering were used (Arensburg and Hershkovitz, 1989). A variety of speculations have been posed regarding the role of plastered skulls in PPNB societies and the possible reasons for their emergence at the time of the development of agriculture (Hershkovitz and Gopher, 1990; Arensburg and Hershkovitz, 1989). Plastered skulls appeared at no other time prior to this period in the history of the Levant.

The interior portion of a plastered skull can neither be inspected visually nor measured. For this reason, previous studies on the subject have been limited in their scope. Computed tomography (CT) and Micro-Focus Radiography (MFR) have

1 Department of Anatomy and Anthropology Sackler School of Medicine Tel Aviv University Ramat Aviv, 69978 ISRAEL.
2 Yoval Goren (PhD) and Nigel Goring Morris (PhD)-Israel Antiquities Authority P.O.B. 586 Jerusalem 91004 ISRAEL.
3 Michael S. Speirs-Department of Sociology & Anthropology Swarthmore College Swarthmore, PA. 19081 USA.
4 Irena Segal-Department of Emission Spectrometry Geological Survey of Israel 30 Malkhei Israel Street Jerusalem 95501 ISRAEL.
5 Oded Meirav and Uri Sherter-ELSCINT Ltd. Advanced Technology Center P.O.B. 550 Haifa, 31004 ISRAEL.
6 Henri Feldman (research assistant)-Department of Non-Destructive Testing Soreq Nuclear Research Center Nahal Soreq Yavne, 70600 ISRAEL.

enabled the study of the internal structures without causing damage to the skulls. In the present paper, we shall describe the use of CT and MFR in the assessment of the internal anatomical structures of the plastered skulls and attempt to reveal some of the plastering techniques.

Materials and Methods

CT and MFR techniques were applied on a newly discovered plastered skull from K'far Hahoresh, a PPNB site in the Upper Galilee, Israel. Although part of the calvaria had collapsed as a result of the earth's pressure, the modeled face showed no visible signs of damage (Fig. 1). The face, zygomatic arches, and skull base as far posterior as the foramen magnum were plastered. No material other than plaster i.e., shell or asphalt was used for decorating or modeling anatomical features. A red pigment coated the skull's modeled face.

CT scans were performed on an ELSCINT 2400 CT installation with a spatial resolution of 0.45 mm and slice thickness of 1.2 mm. To improve resolution, the slice increment was 1.0 mm (overlay of 0.2 mm). The scans were made along a coronal plane. Multi Planner Reformation (MPR) enabled us to examine the skull along any plane desired. One hundred selected scans were used to build a three-dimensional image of the skull. The standard CT numbers which represent the linear attenuation coefficient, were used to identify the different plaster matrix types. In several cases the restricted range of CT numbers enabled us to isolate different parts of the matrix. The range of skull and plaster densities was found to be within the CT limits. We generally followed the guidelines for analysis of skeletal material using computed tomographic (CT) scanning as recommended by Ruff and Leo (1986).

The MFR was carried out on an Andrex MX-3-200 installation with a probe, 375 mm in length and 8 mm in diameter, and radial panoramic X-ray beam output. The probe was inserted into the skull through the foramen magnum. The focus-object distance was 9 cm, focus film distance 18 cm and operation voltage peak near 150 keV and 300mA. A panoramic image of the skull was obtained on X-Ray films (Kodak SR.5). The MFR has two major advantages over conventional X-Ray techniques. First, it can produce highly focused magnified X-ray images; and second, the problem of superimposed structures, which greatly hinders the study of internal morphology in traditional X-Ray, is overcome. Because bone and the plaster matrix have similar chemical and physical properties the problem is even more complex. A conventional X-ray of the face, for example, yields nothing but a large white mass.

Due to the similarity in consistency and chemical properties of both the matrix and the bone as well as the technical limitations of the scanner (slice thickness = 1.2 mm; spatial resolution = 0.45 mm.), we could not isolate the osseous portions of the skull and observe the architecture of the facial skeleton. MFR was

therefore necessary to visualize the general contour of the anatomical landmarks of the face. For this reason, the two methods were used in combination.

RESULTS AND DISCUSSION

A. Visualization of structures covered by plaster matrix.

The coating matrix of most plastered skulls prevents visual inspection of the facial skeleton. CT reveals the cross-sectional details of the bony surface despite the coating matrix. Although the matrix is primarily composed of burnt lime, there is a clear bone-matrix interface (Fig. 2). This enabled us to perform a series of anthropometric measurements (Table 1), in order to confirm a previous hypothesis regarding skull pre-selection according to size and sex (Arensburg and Hershkovitz, 1989). Age and sex of the individual were also estimated from the data provided by CT. We completed our metric analysis on structures which could not be otherwise measured, such as the orbits, using panoramic X-Ray. Thus we obtained a general impression of the skull's shape.

B. Visualization of plaster matrix.

Although the external surface of the plaster appear to be homogenous, coronal horizontal and sagittal CT scans revealed that at least three different units of plaster were applied (Fig. 2 and 3). Using a surgical microscope, we performed a trans-endocranial plaster "biopsy" which enabled us to sample the plaster on various parts of the face without damaging its outer modeled surface. The plaster specimens were subjected to thin-section petrographic analysis (TSPA) as well as chemical analysis. The results clearly show that all three plaster units identified in the CT scans were produced from similar raw materials, and that burnt lime constituted the main component. The different varieties of plaster are the result of different combinations of lime (calcium carbonate) and ash (silica).

The most condensed layer of plaster fills the orbital cavities, infratemporal fossa, base of skull, and hard palate (Figs. 2 and 3), where the ratio of lime to ash is ca. 1:1. In the outer plaster coat, the ratio is ca. 5:1. Different ratios of lime to ash enabled the prehistoric artisan to produce different qualities of plaster which enabled a large degree of freedom in the plaster skull modeling process. Moreover, it appears that the artisan understood that the effects of different quantities of ash on the strength and flexibility of the plaster is not linear, but rather parabolic. Beyond a certain ratio of lime to ash, the physical properties of the plaster change dramatically. It can therefore be concluded that the plaster products were constructed in several stages, and that the various plaster mixtures were intentionally prepared. Despite 8000 years of fluctuating environmental conditions and ground pressure, the plaster has still remained adherent to the skull and the modeled facial features have remained essentially unscathed. The excellent

preservation of the modeling is astonishing when one considers that the weight of the plaster, is more than half a kilogram (the total weight of the plastered skull is 1360 gr.), and that the thickness of the plaster coat in certain areas of the face exceeds 20 mm.

C. Creating a plastered skull

Using CT scans and chemical analysis the different stages of plastering have been identified. Stage 1 : The nasolarimal duct, superior and inferior orbital fissures, optic canal, infraorbital groove and ethmoidal foraminae were obstructed in order to prevent plaster drainage, using a soft material of organic origin (Fig. 3). Stage 2 : The posterior two thirds of the nasal cavity and the maxillary sinuses opening into this cavity were filled with loose plaster (1.3:1 lime to ash) (Fig. 4). An analogous situation in modern-day construction occasionally occurs when architecturally useless spaces are stuffed with paper. The walls of the orbital cavity were coated with soft plaster (Fig. 3). This was probably necessary to insure the stability of the harder matrix which filled much of the orbital cavity. Had the harder plaster, been applied directly to the bone, without an intermediate softer layer, the porous bony substance could have rapidly absorbed the moisture of the plaster. This in turn might have caused the plaster to rapidly dehydrate and crack. Stage 3 : In this stage the bedding was prepared. A large quantity of ash was mixed with burnt lime (about 2 parts lime to 1 part ash) to form a hard, dense material. This was the material which filled the remainder of the orbital cavities, infratemporal region, hard palate, and skull base (Fig. 2). The basicranium was filled to the level of the hard palate in order to create a platform on which the skull could stand (Fig. 5). The foramen magnum was left open. This hard bedding layer probably functioned as the framework to which the outer soft coating adhered. The inner dense layer absorbed water from the external coating, causing these two adjacent layers to stick together. The CT scans clearly reveal that in areas where the bedding material is in contact with the external coating, the two layers cling. In places were the coating is in contact with bone, there is a clear space between the two. It is therefore evident that had the coating layers been directly applied to the bone, the entire structure would most likely have collapsed after a short period of time. Moreover, cracks only appear in places were the plaster was applied directly to the bone.

The mobile mandible and unstable anterior teeth were removed prior to the decoration of the skull (Fig. 6). Stage 4 : A relatively pure (5 : 1) plaster was prepared for modeling the face. In order to create a proportional face, the artisan was compelled to compensate for the missing mandible with plaster. Cranial structures were therefore ignored as the eyes and nose were modeled on the frontal bone, and the mouth at the level of the nasal cavity (Fig. 7 and 8). The anterior-most portion of the floor of the nasal cavity served as a platform to support the massive protruding lips. Three dimensional reconstruction of the hard plaster clearly demonstrates that it formed the framework on which the entire mask rested. Stage 5 : The plaster was painted red. Chemical analysis, Induced Coupled

Plasma-Atomic Emission Spectrometry (ICP-AES), and X-Ray Fluorescence Analysis have identified the pigment as red ochre.

D. The morphological characteristics of the modeled face.

The measurements of the plastered skull appear in Table 1. Plaster thickness on different parts of the face, varied from a few to as many as forty millimeters.

The artisan succeeded in maintaining fairly accurate relations between the various facial structures although the mandible was missing. It should be noted that there were no ears modeled with the plastered face. As can be seen in Figure 1, the eyelids appear to be closed, cheeks are rounded, and mouth appears to be closed and somewhat puckered. In addition, the chin is clefed and no attempt was made to form the impression of a mandible. For these reasons, the face bears some similarity to that of a "sleeping baby".

SUMMARY and CONCLUSIONS

The purpose of this paper was to present some hitherto unavailable technical information on plastered skull construction. Since the internal structures of plastered skulls cannot be directly observed and measured, previous studies have been severely limited. In the present paper we have described the use of CT and MFR to expose the internal anatomy of plastered skulls and reveal some of the plastering techniques employed by ancient artisans. The emergence of plastered skulls at the inception of agriculture suggests that they might have had a ritualistic and/or religious function and served as a socializing factor. The great care taken to create plastered skulls, which entailed skull selection, removal from burial site, plastering, decoration and installation, attest to the importance which might have been ascribed to these artifacts by early farmers. Regional stylistic differences in plastering which were found between sites may have served to distinguish different social groups. Indeed, the PPNB period is known to be an era of great societal upheaval and change.

ACKNOWLEDGMENTS

The authors would like to acknowledge the assistance of the National Center for Collaboration Between the Natural Sciences and Archaeology; Irene Levi Sala Care Foundation; The Israel Antiquities Authority; B. Breitman and T. Karpinovicz of the Soreq Nuclear Research Center; Professor H. Bar Ziv of the Hebrew University Medical School; the Mor Institute, Bnei Brak; and M. Chech of the French Research Mission, Jerusalem.

REFERENCES

ARENSBURG B. and HERSHKOVITZ I., 1989,
Artificial skull "treatment" in the PPNB period: Nahal Hemar. In: I. Hershkovitz (ed.) *People and Culture in Change*. B.A.R. International Series 508, pp.115-132.

BAR-YOSEF O. and BELFER-COHEN A., 1989a,
The Levantine "PPNB" interaction sphere. In (I. Hershkovitz, Ed.) *People and Culture in Change*, Oxford: B.A.R International series, pp. 59-72.

BAR-YOSEF O. and BELFER-COHEN A., 1989b,
The Origins of Sedentism and Farming Communities in the Levant. *Journal of World Prehistory* 3: 447-498.

HERSHKOVITZ I. and GOPHER A., 1990,
Paleodemography, burial customs, and food producing economy at the beginning of the Holocene: A prespective from the southern Levant. *J. Isr. Prehist. Soc.* 23: 9-47.

RUFF C. B. and LEO F. P., 1986,
Use of computed tomography in skeletal structure research. *Yearbook of Physical Anthropology*. 29:181-196.

Measurements		Nasal breadth	24.4
Cranial length	190.5?	Nasion-Prosthion	58.5
Cranial breadth	153.4	Maxillo-alveolar length	53.3
Basion-Nasion	102.7	Maxillo-alveolar breadth	70.6
Po.-Po. breadth	122.5	Palatal length	39.4
Biorbital breadth	103.1	Palatal breadth	33.3
Orbital breadth	32.2	Bizygomatic breadth	137.5
Prosthion-Basion	105.0	Basion-Glabella	110.4
Subnasal clivus length	22.9	Nasal height	37.9
Orbital height	33.0	Maxillo-zygomatic breadth	82.8
Interorbital breadth	27.8	Facial projection	18.5

Table 1: Measurements of the K'far Hahoresh skull from CT images (in mm).

Fig 1 : The modeled skull from K'far Hahoresh. The skull was found within a reconstructed pit, under the plastered floor of a dwelling, at a depth of one meter, together with the complete skeleton of a gazelle.

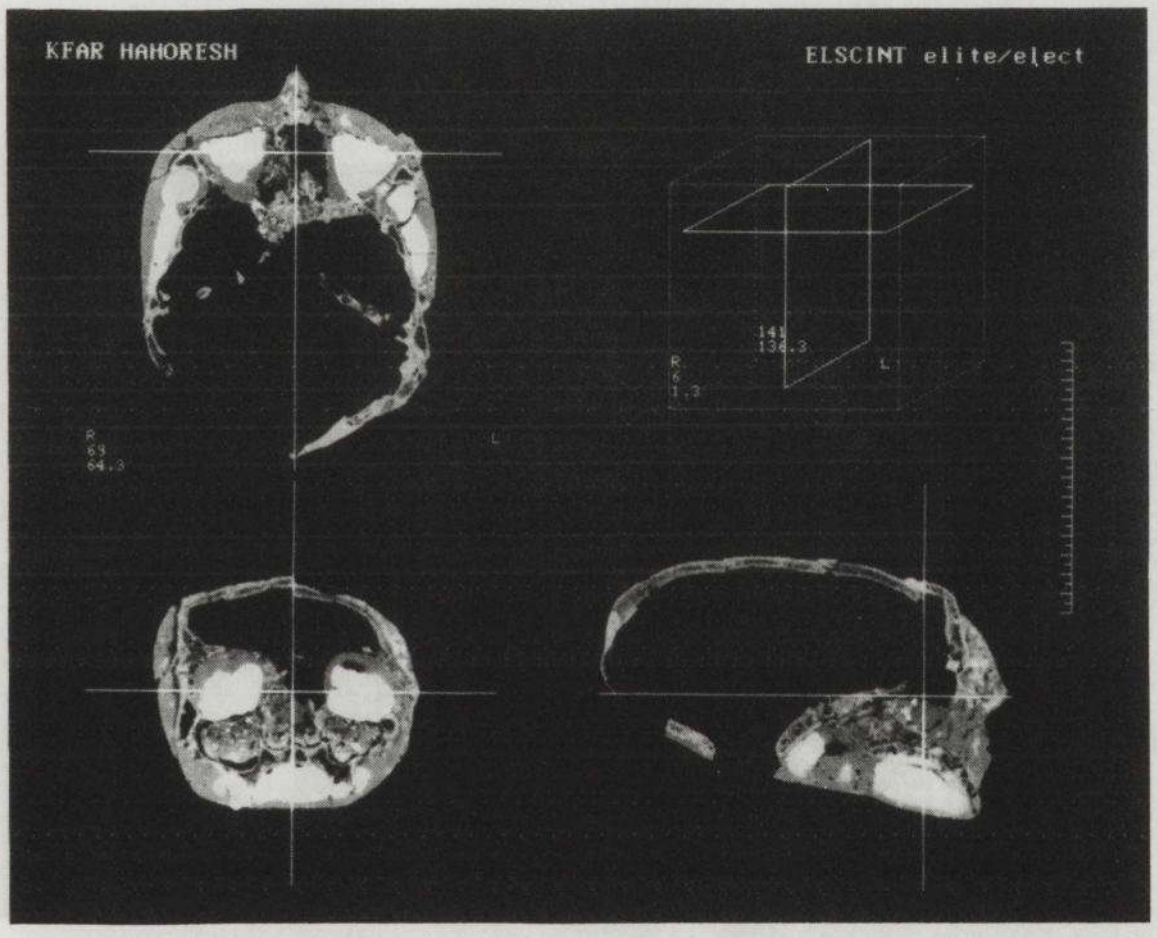

Fig. 2 : Multiplanar sections of K'far Hahoresh modeled skull. Note the varying types of plaster used in different areas: a loose matrix filled the nasal aperture and maxillary sinuses and a hard matrix occupied part of the infratemporal fossa, orbital cavities and hard palate.

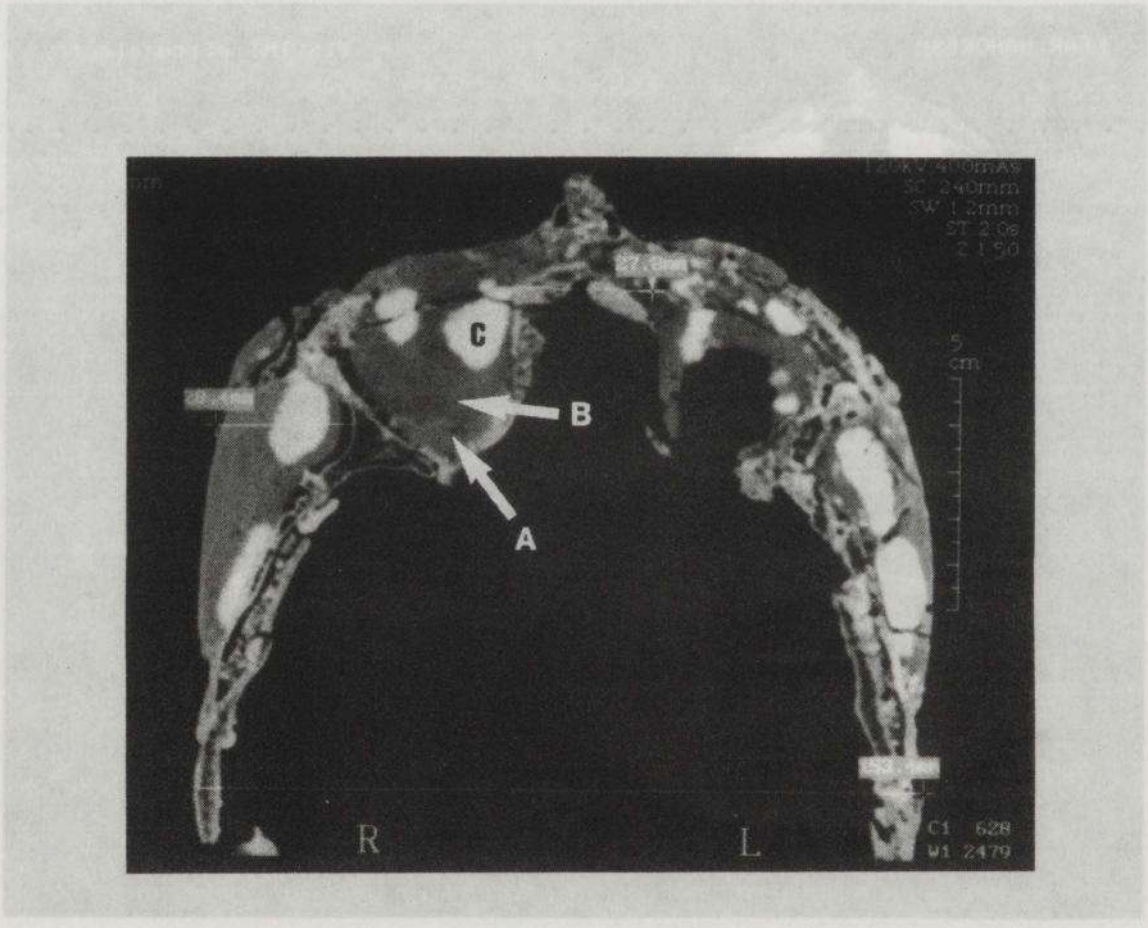

Fig. 3 : Transverse section of K'far Hahoresh skull. Note that the orbital cavity was covered with loose plaster (b) except for it's posterior part which was coated with some sort of organic material (a). Most of the cavity was filled with hard plaster (c) (here seen only in the apex of the orbital cavity).

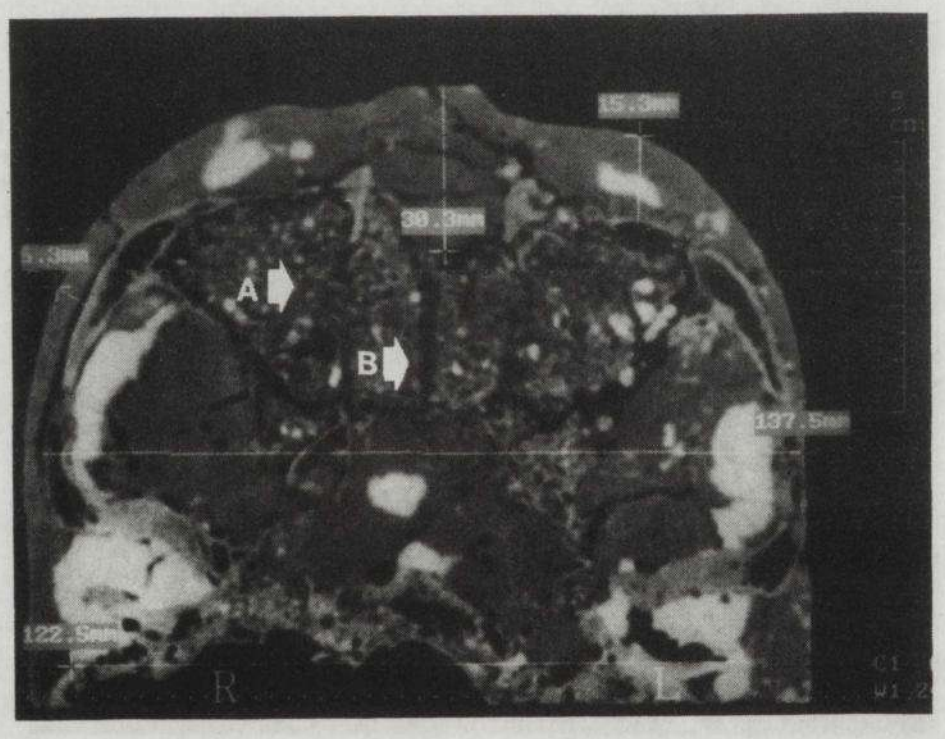

Fig. 4 : Transverse section of the skull at the level of the zygomatic arch. Note the granular plaster filling the maxillary sinus (a) and the middle and posterior nasal cavity.

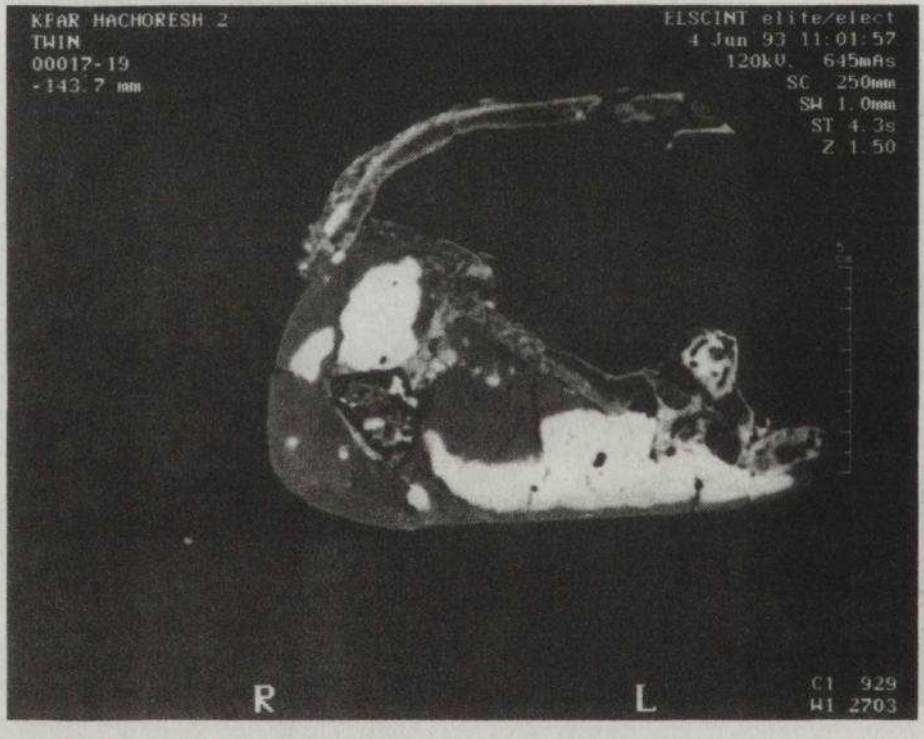

Fig. 5 : Parasagittal section of the modeled skull. Note that the base of the skull was coated with hard plaster on which the skull could rest.

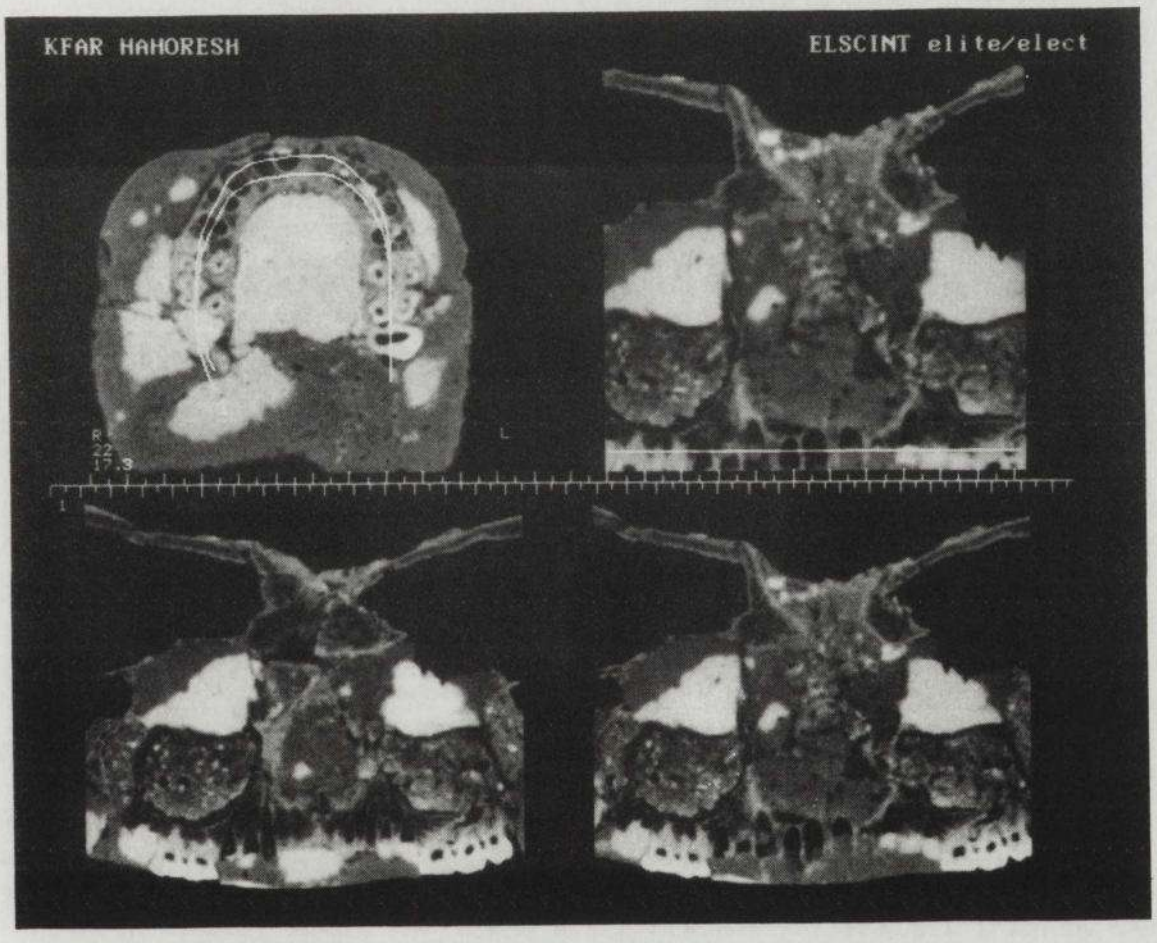

Fig. 6 : Panoramic view of the maxilla. Note that all teeth excluding the molars were extracted prior to decoration of the skull.

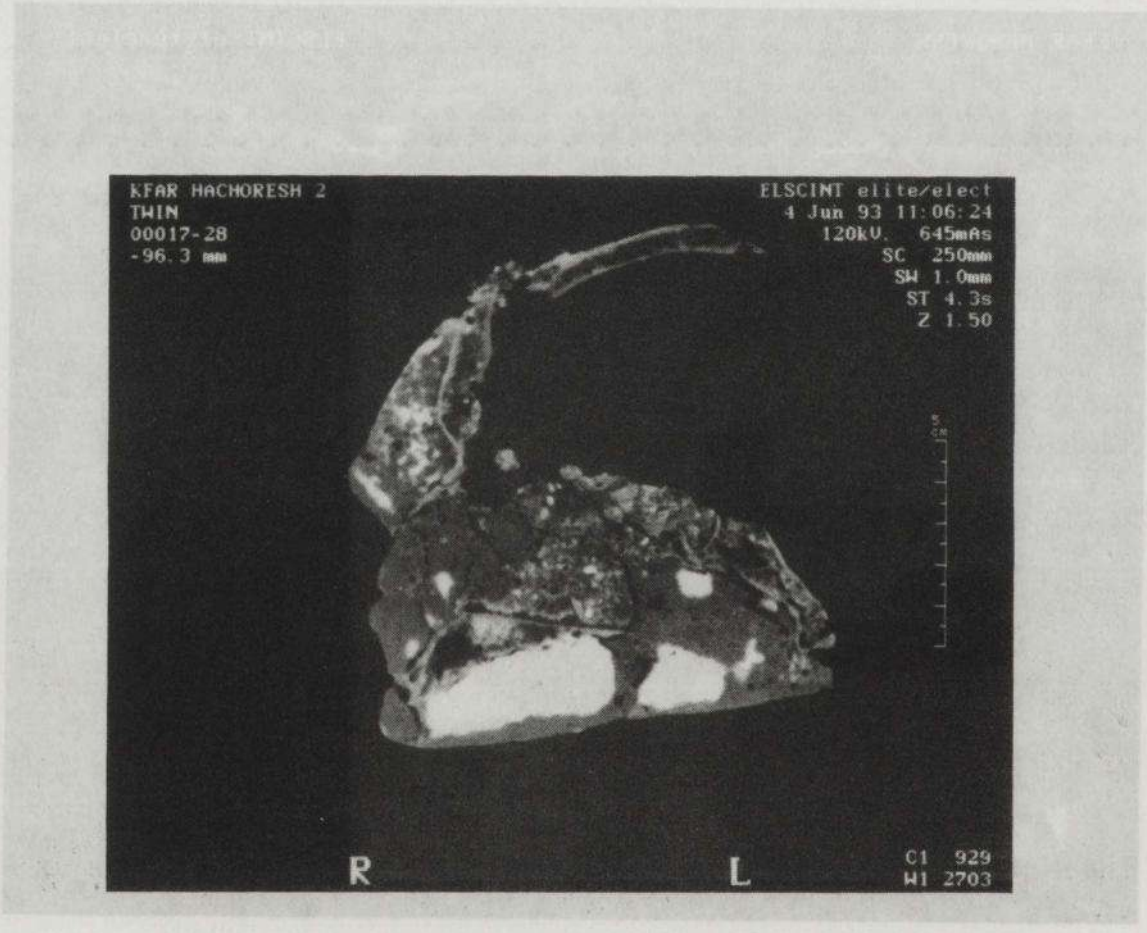

Fig. 7 : Midsagittal section of the modeled face. Most of the modeled nose is located on the frontal bone. The lips lie anterior to the nasal aperture and the mentum is carved plaster which lies anterior to the nasal clivus.

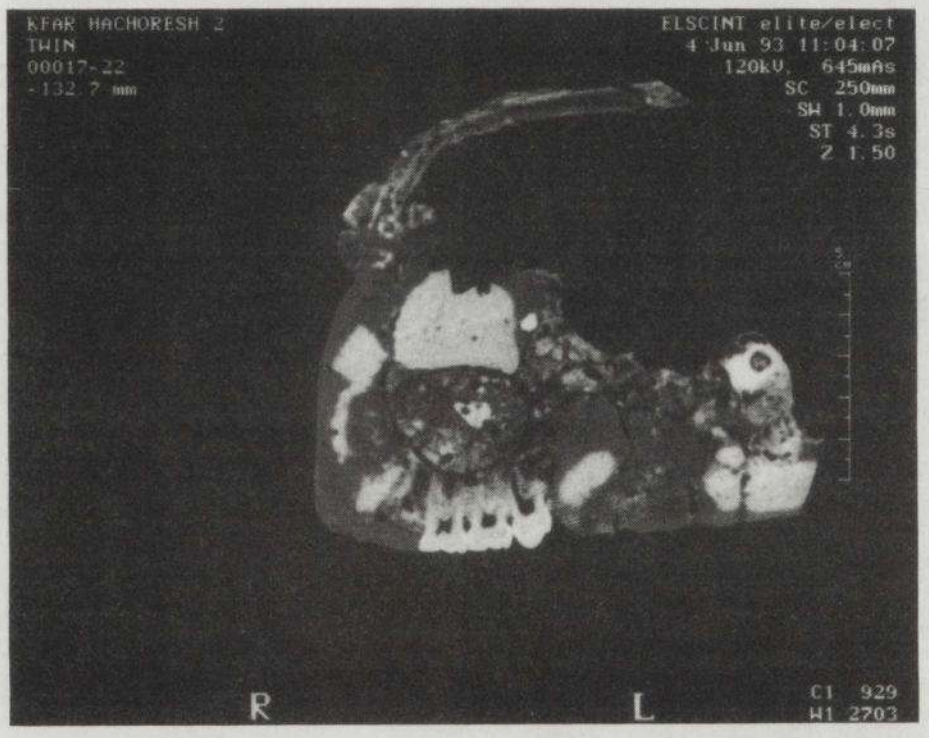

Fig. 8 : Parasagittal section through the modeled eye. Note the discrepancies between the modeled face and the actual facial skeleton.